

# Spatial stress fluctuations: acoustic evidence and numerical simulations

A. Niemunis, T. Wichtmann & Th. Triantafyllidis

*Institute of Soil Mechanics and Foundation Engineering, Ruhr-University Bochum*

**ABSTRACT:** The evolution of the spatial fluctuation of stress in granular materials under cyclic loading was studied both experimentally and numerically. In the FE calculations a random initial stress field was generated and a modern high-cycle model was used to study its evolution during cyclic loading. The distribution of stress was found to be smoothed by the cycles. The purpose of model tests was to determine the spatial stress fluctuation from measurements of acoustic emissions during a bearing capacity test with a foundation on a fine gravel. The same initial density was achieved either by pluviation or by cyclic preloading. Interestingly, no dependence of the intensity of acoustic emission on cyclic preloading could be found.

## 1 INTRODUCTION

The initial spatial fluctuations of stress are expected to be smoothed by a high-cyclic loading (i.e. a loading with a large number of cycles but small amplitudes  $\varepsilon^{\text{ampl}} < 10^{-3}$ ). According to the Hertz contact formula, a smooth distribution of stress should be energetically advantageous. We put this hypothesis into question.

The registration of acoustic emission (AE) provides a qualitative estimation of the intensity of grain crushing or contact rearrangements and hence one may speculate about the presence of strong stress peaks. It is well known (Oda and Iwashita 1999) that the acoustic emission becomes intensive during loading whereas during unloading or reloading almost nothing is received. Here we attempt to use the acoustic emission in order to detect the stress peaks in the subsoil of a model foundation and to distinguish between homogeneous and strongly inhomogeneous stress fields. The load-displacement curve and the intensity of acoustic emission are therefore registered for the following two cases: a) freshly pluviated granular material b) loosely pluviated and subsequently densified (by cyclic loading) granular material. At identical void ratios, the material with cyclic preloading was expected to have fewer stress peaks and to cause less noise during loading.

The evolution of the spatial fluctuation of stress during cyclic loading was also tested numerically using the high-cycle model recently proposed by the authors (Niemunis et al. 2005) and the FE program ABAQUS. Spatially correlated fluctuation fields have

been generated and subject to cyclic loading.

Finally, the evolution of stress concentrations during cyclic loading in the experiments and in the FE calculations are compared.

## 2 RANDOM MODELLING OF SOIL AND FE CALCULATIONS

Various properties of soil may be considered as random. In the present work, the void ratio  $e$  and stress  $\mathbf{T}$  are of primary interest. Their scatter over a certain volume of soil is modelled by random fields discretized on the FE mesh.

### 2.1 Random void ratio

In order to generate a scalar random field of the void ratio, we need the estimates of its characteristic values, e.g. the mean, the variance and the spatial correlation. Such estimates may be extracted from in-situ measurements. For example, the mean of the respective parameter of a known sample of  $n$  measurements reads

$$E[\sqcup] = \frac{1}{n} \sum_{i=1}^n \sqcup_i. \quad (1)$$

Alternatively a maximum likelihood estimator (MLE) could be used, (DeGroot and Beacher 1993; Fenton 1999). The estimator should be *unbiased* (the estimated average of a population is equal to the mean of the measured sample) and *consistent* (the dispersion decreases with the size of a sample i.e. the number of measurements).

First let us examine the void ratio  $e$  at a given point  $\mathbf{x}$  in space. For a fictitious subsoil considered here, the mean void ratio is assumed to be  $\bar{e} = 0.8$  and the probability density function (PDF) is chosen to be constant and equal to  $1/0.4$  over the  $e$ -range from 0.6 to 1.0, i.e.  $\sigma^2 = 0.04/3$ . We do not use the normal Gaussian distribution here because extremely small or extremely large void ratios may cause problems in the constitutive models. Moreover, negative void ratios are physically impossible.

Let us suppose, we have a statistical sample of  $n$  measurements of  $e$  taken at various locations  $\mathbf{x}_i$  with  $i = 1, \dots, n$  and the void ratio at a point  $\mathbf{x}_i$  is related to the void ratio at a point  $\mathbf{x}_j$ . For all  $m$  pairs  $(i, j)$  of points  $\mathbf{x}_i, \mathbf{x}_j$  of a given statistical sample (set of  $n$  measurements) lying at a given distance  $d$  we may quantify the difference of the void ratios. Furthermore, let this difference be isotropic, i.e. independent of the orientation of the vector  $\mathbf{x}_i - \mathbf{x}_j$ . Having measured the void ratio  $e(\mathbf{x})$  over some area we can distinguish its trend  $\bar{e}(\mathbf{x})$  (a mean value, often estimated by linear regression) and scatter  $\tilde{e}(\mathbf{x})$ :

$$e(\mathbf{x}) = \bar{e}(\mathbf{x}) + \tilde{e}(\mathbf{x}). \quad (2)$$

For simplicity, we assume that the void ratio does not decrease with the depth, i.e. the trend to be equal to the mean,  $\bar{e}(\mathbf{x}) = 0.8$ . The autocorrelation of the scatter  $\tilde{e} = e - \bar{e}$  could be evaluated from measurements using the moment estimate of the isotropic autocovariance of  $\tilde{e}$ . For a typical pair of points at distance  $d$  it is

$$\rho(\tilde{e}(\mathbf{x}), d) = \frac{1}{\sigma^2 m} \sum_i^n \sum_j^n \tilde{e}(\mathbf{x}_i) \tilde{e}(\mathbf{x}_j) w(\mathbf{x}_i, \mathbf{x}_j), \quad (3)$$

$$\text{wherein } w(\mathbf{x}_i, \mathbf{x}_j) = \begin{cases} 1 & \text{if } \|\mathbf{x}_i - \mathbf{x}_j\| \approx d \\ 0 & \text{otherwise} \end{cases},$$

$n$  is the total number of points and  $m(d) = \sum_i^n \sum_j^n w(\mathbf{x}_i, \mathbf{x}_j)$ .

For our fictitious subsoil we assume the Markovian (exponential) spatial correlation function between the void ratios  $\tilde{e}$  at points  $\mathbf{x}_i$  and  $\mathbf{x}_j$  at distance  $d = \|\mathbf{x}_i - \mathbf{x}_j\|$  according to

$$\rho(\tilde{e}, d) = \exp(-d/\theta), \quad (4)$$

wherein  $\theta$  denotes the correlation length.

Soil properties may vary at many scales (fractally) so the value of  $\theta$  depends on the size of the problem. Using the estimations of  $\theta$  from the literature one should select a correlation length estimated on a similar soil over a domain of a similar size (Fenton and Griffith 2002). Of course, we have to choose a value between the limit cases  $\theta \rightarrow 0$  and  $\theta \rightarrow \infty$  for which the void ratios are either fully uncorrelated

(statistically independent) or perfectly correlated, respectively. Some recommendations for the choice of  $\theta$  were given by (Fenton and Griffith 2002). In the numerical examples presented further  $\theta = 0.02$  m was chosen.

In the FE calculations quadrilateral elements with four Gauss integration points were used. Various possibilities of random field discretization are reported in the literature (Matthies et al. 1997). For simplicity reasons, we discretize the random field of void ratios  $e$  by the FE mesh using the mentioned Gauss points.

The field variability is described by the following isotropic autocorrelation function:

$$C_{ij} = \sigma^2 \exp\left(-\frac{d_{ij}}{\theta}\right) \quad (5)$$

with

$$d_{ij} = \|\mathbf{x}_i - \mathbf{x}_j\|, \quad (6)$$

$$\sigma = \frac{1}{2\sqrt{3}}(e_{\max} - e_{\min}), \quad (7)$$

and  $e_{\max} = 1.0$ ,  $e_{\min} = 0.6$ .

This matrix  $\mathbf{C}$  is then transformed to the uncorrelated space by the orthogonal transformation (spectral decomposition) based on its eigenvalues  $\Lambda = \text{diag}\{\lambda_1, \dots, \lambda_n\}$  and an orthogonal matrix  $\Phi$ ,

$$\mathbf{C} = \Phi \cdot \Lambda \cdot \Phi^T. \quad (8)$$

The matrix  $\Phi$  is composed of orthonormalized eigenvectors (in columns, numbering same as for  $\lambda$ -s),  $\Phi = \{\Phi_1, \dots, \Phi_n\}$ .

The field  $\tilde{e}(\mathbf{x})$  is generated by using all eigenvalues (although (Novak et al. 2001) suggests using only a few largest ones) and the corresponding eigenvectors  $\Phi_i$ ,  $i = 1, \dots, n$  multiplied by random factors, viz.

$$\tilde{e}(\mathbf{x}) = \sum_{i=1}^n r_i^{[-1,1]} \frac{1}{2} \sqrt{\lambda_i} \Phi_i \quad (9)$$

wherein  $r^{[-1,1]}$  is a uniform variate (random real number with constant PDF) from the range  $[-1, 1]$  and  $\lambda_i$  is the  $i$ -th eigenvalue of  $\mathbf{C}$ . Of course one may easily find  $r^{[-1,1]} = 2r^{[0,1]} - 1$  using the intrinsic random function  $r^{[0,1]}$  provided in all programming languages. The final field of void ratios is obtained from (2).

A set of  $N_{\text{sim}}$  fields (=simulations)  $\tilde{e}(\mathbf{x})$  could be generated directly using (9), with random  $r^{[-1,1]}$  (=Monte Carlo method). We usually apply a so-called Latin Hypercube Sampling (LHS), (Florian 1992) to enforce the full range of variability of the void ratios with smaller number of simulations.

## 2.2 Evolution of the fluctuation of the void ratio

Under homogeneous stress conditions the cyclic loading must lead to smoothing of spatial fluctuations of the void ratio because loose sand densifies faster than dense sand.

It is possible to observe the evolution of the fluctuation of the void ratio of a sand sample directly from the analysis of X-ray images. However, it is much easier to observe the fluctuation of the *changes* of volume or generally of the increments of strains. Such study with the particle image velocimetry technique (PIV) was used by (Niemunis 2003) to find the smoothing effect of the cyclic preloading (40 000 cycles) on the spatial fluctuation of subsequent strain increments. Contrarily to the theoretical tendency to spontaneous smoothing no such effect could be observed, neither in the rate of strain accumulation nor in the amplitude.

## 2.3 Random geostatic stress field

Some mechanical properties of soil may be related to the number of the force chains between individual grains of soil which contribute to the transfer of the applied load. At a given pressure and a void ratio we may consider a situation with few chains but each carrying large forces or a situation with many moderately loaded chains. The behaviour of soil is expected to be different in both situations.

Our aim is to express this micro-mechanical difference by the spatial fluctuation of stress using the FE techniques. The total stress  $\mathbf{T}$  is assumed to consist of its trend (volume average)  $\bar{\mathbf{T}}$  and its fluctuation  $\tilde{\mathbf{T}}$

$$\mathbf{T} = \bar{\mathbf{T}} + \tilde{\mathbf{T}} \quad \text{with} \quad \langle \tilde{\mathbf{T}} \rangle = \mathbf{0} \quad (10)$$

where  $\langle \rangle$  denotes volume averaging.

One method to add spatial fluctuations to the initial stress field is to variate the individual components of stress  $T_{ij}(\mathbf{x})$  about the geostatic stress treated as a trend. All components were generated independently as spatially correlated scalar random fields. The fluctuation was not strong so that the yield criterion by Matsuoka & Nakai (M-N criterion) (Matsuoka and Nakai 1977)

$$y \equiv \text{tr} \mathbf{T} \text{tr} \mathbf{R} - \phi < 0 \quad (11)$$

$$\text{with} \quad \mathbf{R} = \mathbf{T}^{-1} \quad \text{and} \quad \phi = \frac{9 - \sin^2 \varphi}{1 - \sin^2 \varphi} = 0$$

was satisfied everywhere ( $\varphi$  denotes the friction angle and  $\text{tr} \mathbf{T} \text{tr} \mathbf{R} = I_1 I_2 / I_3$ ). However such "rough" stress field (e.g. Fig. 1a) was not in equilibrium and has to undergo the equilibrium iteration procedure (an initial stress problem in FE). In the redistributed stress field (Fig. 1b, obtained after a direct equilibrium iteration with an elastoplastic model with M-N-criterion

of  $\varphi = 25^\circ$  and small stiffness:  $E = 500$  kPa,  $\nu = 0$ ) the initial fluctuations are slightly smoothed. The pattern of the fluctuation does not correspond to the FE discretization (no mesh alignment) presumably due to the spatial correlation of the disturbance. Note, however, that our equilibrated self-stress results from the low order of the shape functions within the FE and from the stress jumps on the element borders rather than from the true (physical) incompatibility of the strain field

$$\tilde{T}_{ij} = E_{ijkl} \tilde{\epsilon}_{kl} \quad (12)$$

$$\text{with} \quad e_{akr} e_{bls} \tilde{\epsilon}_{kl,rs} = -\eta_{ab} \quad \text{and} \quad \tilde{T}_{ij,j} = 0_i$$

where  $e_{bls}$  is the permutation symbol and  $\eta_{ab}$  is an arbitrary tensor of strain incompatibility. A random generation of the field  $\eta_{ab}(\mathbf{x})$  to obtain  $\tilde{T}_{ij}(\mathbf{x})$  from (12) would necessitate a higher order smoothness of the strain field which might be difficult within the framework of a conventional FE analysis. Therefore we do not generate the stress fluctuations basing on the strain incompatibility.

Another method to add spatial fluctuations to the initial stress field is to generate a random *stiffness* field and then to apply the self weight. Both elastic parameters  $\nu, E$  can be varied (usage of anisotropic elasticity would be of interest). The trend of stiffness  $E$  is chosen to increase with depth and the trend of Poisson ratio  $\nu = \frac{1}{3}$  renders  $K_0 \approx \frac{1}{2}$  as desired. Admittedly the procedure is artificial (does not reproduce any pluviation or sedimentation process) but we are interested solely in the final stress field. Although the resulting stress field is in equilibrium it does not necessarily satisfy (11). Therefore, similarly as in the previously described method our stress field should undergo the equilibrium iteration procedure, a direct initial stress problem using the elastoplastic model. As previously no mesh alignment was observed.

Yet another possibility to introduce stress fluctuation into a constitutive model could be its description by an additional state variable which does not appear directly in the equilibrium condition but influences stiffness and the evolution of stress. We may assume that the equilibrium condition need to be satisfied by the average stress (without fluctuations) only and do not bother about the equilibrium on the micro-level. Suppose we choose a plane cross-section in soil which intersects many force chains. Our interest is not the average stress vector but the variability of force from one force chain to another. This variability may depend on the orientation of our cross-section so it can conveniently be expressed by a directional (tensorial) variable. Formulation of relevant structure tensors is discussed e.g. by Kanatani (Kanatani 1981; Kanatani 1984; Kanatani 1985). The so-called intergranular strain (Niemunis and Herle 1997) or the back

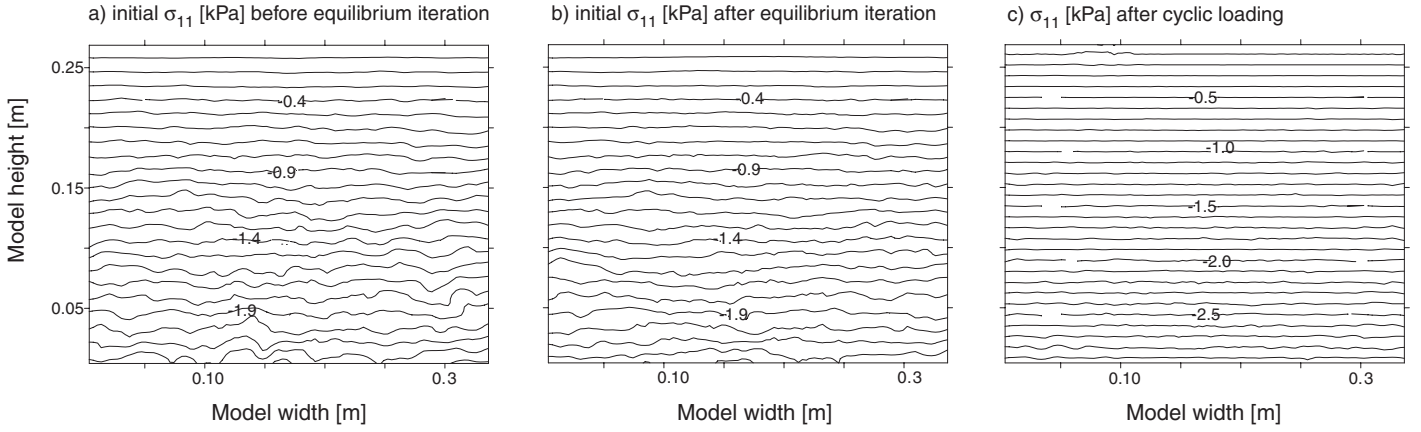


Figure 1. Contours  $T_{11} = \text{const}$  a) obtained from the rough stress field generated with randomness proportional to the mean pressure, b) after the rough field has been brought to equilibrium obeying the M-N yield criterion, c) smoothed in the course of cyclic loading. The equilibrium condition and the M-N yield criterion are satisfied.

stress can be interpreted using such variability (Gudehus 2007).

The final remark in this section concerns the elastic energy of the spatially fluctuating stress field. It has been shown (Triantafyllidis and Niemunis 2000; Niemunis 2003) that according to the Hertz contact formula, a smooth distribution of stress should be energetically advantageous. Therefore one can expect a spontaneous smoothing of the fluctuations in soil. The Hill's condition (used in homogenization) states that the power densities on the micro- and the macro-level are identical, i.e.  $\langle \mathbf{T} : \mathbf{D} \rangle = \langle \mathbf{T} \rangle : \langle \mathbf{D} \rangle$ , where  $\langle \cdot \rangle$  denotes averaging over the same volume. This condition holds for either uniform boundary tractions or linear boundary displacements (Nemat-Nasser and Hori 1993) independently of the material model. Hence, in these cases the Hill's condition contradicts the conclusion (Triantafyllidis and Niemunis 2000; Niemunis 2003) about the spontaneous smoothing.

#### 2.4 Evolution of stress fluctuation during cyclic loading

Judging by the constitutive equations of our high-cycle model (Niemunis et al. 2005) describing the intensity of the accumulation one cannot easily predict the evolution of the stress fluctuation. On one hand the deviatoric stress peaks increase the accumulation which has a smoothing effect but on the other hand the rate of accumulation is larger at lower mean pressure which leads to a positive feed-back effect. The mean pressure should quickly decrease where it is low already. Hence the fluctuations in the mean pressure should grow. From the numerical example we conclude that the first phenomenon prevails and the fluctuations dwindle with the number of cycles.

In the presented example 100 cycles with a uniform strain amplitude of 0.05% were applied to the numerical model. The fluctuations of the initial stress have been significantly smoothed in the course of such

cyclic loading. This effect is evident from Figures 1b and 1c.

### 3 MODEL TESTS WITH ACOUSTIC EMISSION MEASUREMENTS

Crushing of grains or chipping of the grain edges or changes in contacts occur at large stress ratios and produce acoustic emissions (AE). A strong spatial stress fluctuation goes together with a large number of locations with high stress ratios and should thus lead to larger rates of AEs. We have compared the AEs of freshly pluviated and cyclically preloaded granular material in model tests with a strip foundation which was subjected to a monotonic displacement-controlled loading (bearing capacity test). A scheme is presented in Figure 2.

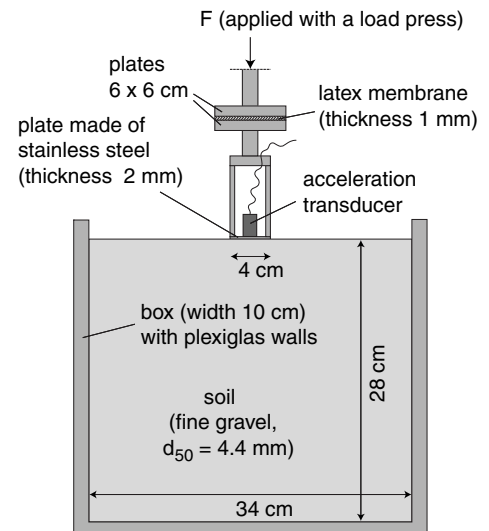


Figure 2. Scheme of the model test

As confirmed by preliminary tests, the intensity of AEs increases with increasing mean diameter of the grains. Thus, all tests were performed on a fine gravel (mean grain diameter  $d_{50} = 4.4$  mm, non-uniformity coefficient  $C_u = d_{60}/d_{10} = 1.3$ , subangular

grain shape, minimum void ratio  $e_{\min} = 0.669$ , maximum void ratio  $e_{\max} = 0.851$  according to German Standard Code DIN 18126). The grain size distribution curve is given as curve No. 6 in Figure 4.14 in (Wichtmann 2005).

The testing program is summarized in Table 1. Except test No. N1 (where the fine gravel was placed with a spoon) the test material was pluviated out of a funnel. Seven tests (Nos. N1 to N7) were performed on such "freshly pluviated" material, i.e. without cyclic preloading. In six other tests (Nos. P1 to P6) the soil was placed in approx. 3 cm thick, originally loose layers ( $I_D = (e_{\max} - e)/(e_{\max} - e_{\min}) \approx 0.22$ ) and afterwards each layer was compacted by vibration, i.e. a certain number of blows against the walls of the model test box using a rubber hammer.

Table 1. Testing program ( $I_{Dp}$ ,  $I_{D0}$  = relative densities after pluviation and prior to the bearing capacity test)

Test No.	$I_{Dp}$	Compaction: Hits per layer	$I_{D0}$
N1	0.22	-	0.22
N2	0.22	-	0.22
N3	0.60	-	0.60
N4	0.77	-	0.77
N5	0.88	-	0.88
N6	1.06	-	1.06
N7	1.12	-	1.12
P1	$\approx 0.22$	4	0.55
P2	$\approx 0.22$	10	0.69
P3	$\approx 0.22$	20	0.89
P4	$\approx 0.22$	20	0.91
P5	$\approx 0.22$	40	1.04
P6	$\approx 0.22$	40	1.04

The model foundation was placed on the soil surface without embedding. A gap of approximately 0.5 mm maintained between the walls of the model test box and the foundation in order to keep friction as small as possible. The plexiglas walls of the model test box had a sufficient thickness to keep lateral deformations small.

The bottom of the model foundation (width 4 cm) consisted of a thin steel plate (thickness 2 mm) on which an AE transducer of the accelerometer type was fixed. Its signal was amplified and sampled continuously with a frequency of 10 kHz. Also the axial load and the axial displacement were measured. Guidance of the foundation in the axial direction was achieved by two plates ( $6 \times 6$  cm) separated by a membrane for isolating the foundation from noise generated by the load press. The displacement-controlled loading was applied with a velocity of 5 mm/min.

Figure 3 presents the record of acceleration during test No. P5 and Figure 4 shows a zoom of three AE events. The AE events were counted using the "Event Count Method" (Oda and Iwashita 1999). The duration of an AE event was usually less than 0.005 s. The

cumulative number of AE events is denoted as  $N_{AE}$ . The amplitude  $A_{AE}$  of an AE event was defined as the largest absolute value of acceleration (Fig. 4). AE signals with amplitudes lower than  $0.5 \text{ m/s}^2$  were treated as background noise and thus were ignored. The rate of AE events  $\dot{n}_{AE} = \Delta N_{AE} / \Delta t$  was calculated using a time period of  $\Delta t = 5$  seconds.

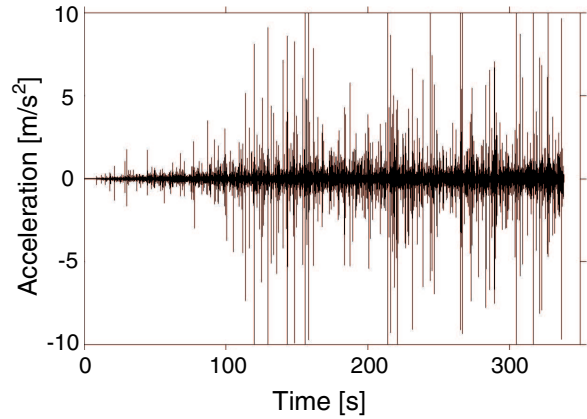


Figure 3. Acoustic emission during test No. P5

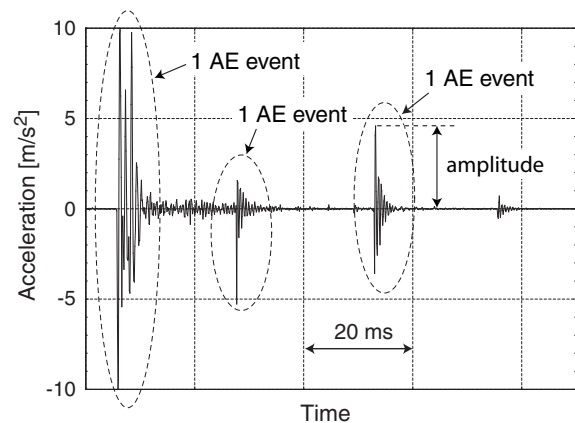


Figure 4. Typical acoustic emission signals during test No. P5

The exemplary diagrams in Figures 5, 6 (tests without cyclic preloading) and Figures 7 to 8 (tests with cyclic preloading) present the external force  $F$ , the square of the amplitude  $(A_{AE})^2$  divided by noise ( $= 0.5 \text{ m/s}^2$ ), the rate  $\dot{n}_{AE}$  and the average amplitude  $\bar{A}_{AE} = \Delta \sum A_{AE} / \Delta N_{AE}$  during a time period  $\Delta t = 5$  seconds as functions of settlement. Interestingly, the most pronounced AE events with large amplitudes seem not to correlate with significant drops in the curve of external load. The rate  $\dot{n}_{AE}$  increases with the applied load  $F$  due to increased stress ratios in the soil. As the bearing capacity also the rate  $\dot{n}_{AE}$  increases with increasing initial density  $I_{D0}$ . The average amplitude  $\bar{A}_{AE}$  seems to be almost independent of  $F$  and  $I_{D0}$ .

Figure 9 shows the cumulative count of AE events  $N_{AE}$  for six tests, three of them were performed with freshly pluviated material and three other ones with

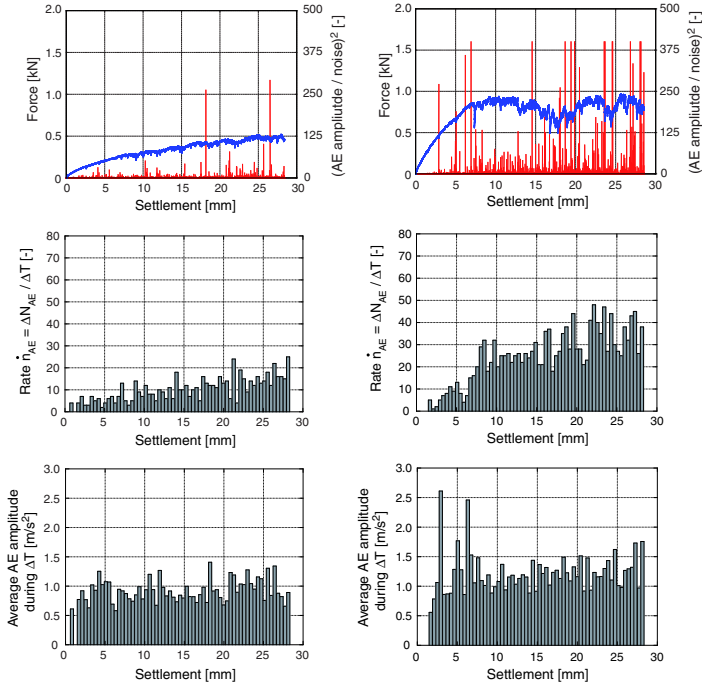


Figure 5. Test No. N2 ( $I_{D0} = 0.22$ ) Figure 6. Test No. N5 ( $I_{D0} = 0.88$ )

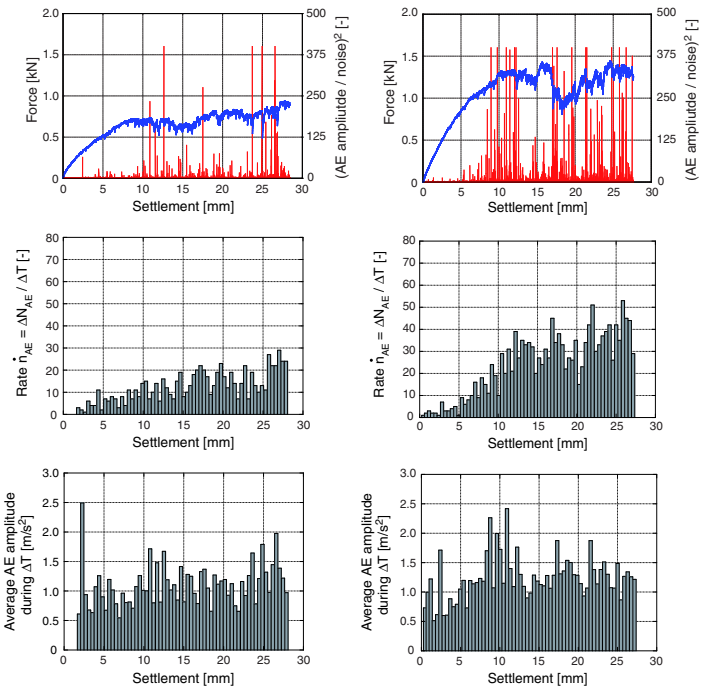


Figure 7. Test No. P2 ( $I_{D0} = 0.69$ ) Figure 8. Test No. P5 ( $I_{D0} = 1.04$ )

cyclically preloaded soil. Figure 10 presents an analogous diagram for  $\sum A_{AE}$ . The shape of the curves in these two figures seems not to depend on cyclic preloading.

The values  $N_{AE}$  and  $\sum A_{AE}$  at a settlement of  $s = 20$  mm were plotted as a function of the initial relative density in Figures 11 and 12, respectively. The data points from the tests with cyclic preloading do not vary significantly from those obtained in the tests on freshly pluviated material. Thus, the rate and the amplitude of AE events seem not to depend on cyclic

preloading. Therefore, the experiments provide evidence that the initial spatial stress fluctuation is independent on cyclic preloading.

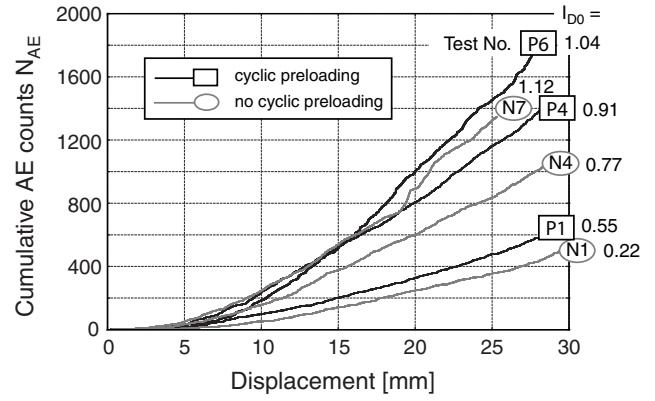


Figure 9. Cumulative count of AE events  $N_{AE}$  for six tests

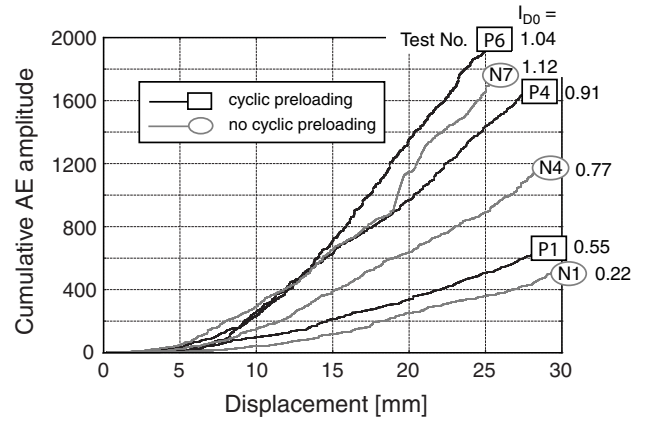


Figure 10. Cumulative amplitude  $\sum A_{AE}$  for six tests

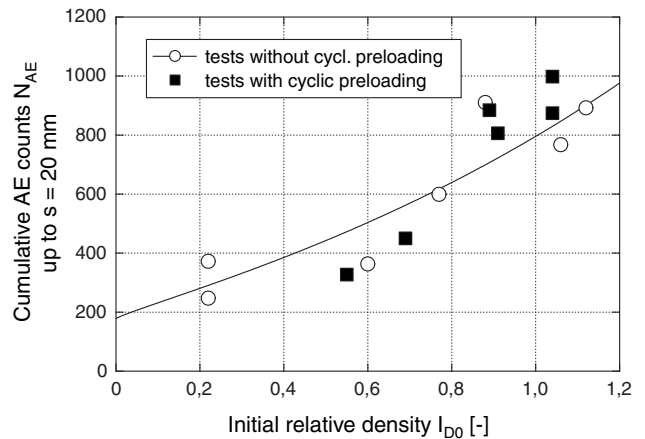


Figure 11. Cumulative count of AE events  $N_{AE}$  at a settlement  $s = 20$  mm as a function of initial relative density  $I_{D0}$

#### 4 CONCLUSIONS

FE calculations with random initial stress fields using a high-cycle model gave evidence that cyclic loading leads to a smoothing of the spatial stress fluctuations. A simple bearing capacity test was used to detect the

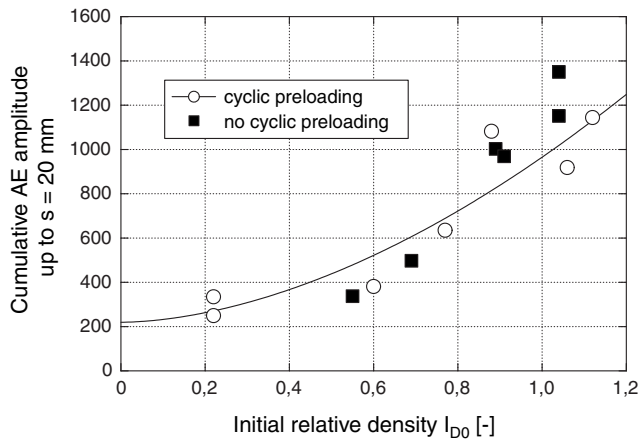


Figure 12. Cumulative amplitude  $\sum A_{AE}$  at a settlement  $s = 20$  mm as a function of initial relative density  $I_{D0}$

inhomogeneities in the stress experimentally. At first we expected that a cyclic preloading of the subsoil would smooth the stress field in the subsoil and for the same void ratio and same load we would obtain less settlement and less acoustic emission. The tests performed with a physical 1-g model of relatively small dimensions with a strip foundation pressed into the soil have shown almost identical load-displacement curve and identical intensities of the acoustic emission independently of cyclic preloading.

## 5 ACKNOWLEDGEMENTS

The authors are grateful to DFG (German Research Council) for the financial support. This study is a part of the project A8 "Influence of the fabric changes in soil on the lifetime of structures" of SFB 398 "Lifetime oriented design concepts".

## REFERENCES

- DeGroot, D. and G. Becher (1993). Estimating autocovariance of in-situ soil properties. *Journal of Geotechnical Engineering, ASCE* 119(1), 147–166.
- Fenton, G. (1999). Estimation for stochastic soil models. *Journal of Geotechnical and Geoenvironmental Engineering, ASCE* 125(6), 470–484.
- Fenton, G. and D. Griffith (2002). Probabilistic foundation settlement on spatially random soil. *Journal of Geotechnical and Geoenvironmental Engineering, ASCE* 128(5), 381–390.
- Florian, A. (1992). An efficient sampling scheme: Updated latin hypercube sampling. *Probabilistic Engineering Mechanics* 2(7), 123–130.
- Gudehus, G. (2007). *Physical Soil Mechanics*. Springer (in print).
- Kanatani, K.-I. (1981). A theory of contact force distribution in granular materials. *Powder Technology* 28, 167–172.
- Kanatani, K.-I. (1984). Distribution of directional data

and fabric tensor. *International Journal of Engineering Science* 22, 149–160.

- Kanatani, K.-I. (1985). Procedures for stereological estimation of structural anisotropy. *International Journal of Engineering Science* 23(5), 587–598.
- Matsuoka, H. and T. Nakai (1977). Stress-strain relationship of soil based on the smp, constitutive equations of soils. In S. Murayama and A. Schofield (Eds.), *Speciality Session 9*. Japanese Society of Soil Mechanics and Foundation Engineering. IX ICSEMF, Tokyo.
- Matthies, H., C. E. Brenner, C. G. Bucher, and C. Soares (1997). Uncertainties in probabilistic numerical analysis of structures and solids - Stochastic finite elements. *Structural Safety* 19(3), 283–336.
- Nemat-Nasser, S. and M. Hori (1993). *Micromechanics: Overall Properties of Heterogeneous Solids, 1st Edition*. Elsevier Science Publishers.
- Niemunis, A. (2003). Extended hypoplastic models for soils. Habilitation, Veröffentlichungen des Institutes für Grundbau und Bodenmechanik, Ruhr-Universität Bochum, Heft Nr. 34. available from [www.pg.gda.pl/~aniem/an-liter.html](http://www.pg.gda.pl/~aniem/an-liter.html).
- Niemunis, A. and I. Herle (1997). Hypoplastic model for cohesionless soils with elastic strain range. *Mechanics of Cohesive-Frictional Materials* 2, 279–299.
- Niemunis, A., T. Wichtmann, and T. Triantafyllidis (2005). A high-cycle accumulation model for sand. *Computers and Geotechnics* 32(4), 245–263.
- Novak, D., W. Lawanwisut, and C. Bucher (2001). Simulation of random fields based on orthogonal transformation of covariance matrix and Latin Hypercube Sampling. In G. Schueller and P. Spanos (Eds.), *Monte-Carlo Simulation*, pp. 129–136. Balkema.
- Oda, M. and K. Iwashita (1999). *Mechanics of Granular Materials*. Balkema, Rotterdam.
- Triantafyllidis, T. and A. Niemunis (2000). Offene Fragen zur Modellierung des zyklischen Verhaltens von nichtbindigen Böden. In *Beiträge zum Workshop: Boden unter fast zyklischer Belastung: Erfahrungen und Forschungsergebnisse, Veröffentlichungen des Institutes für Grundbau und Bodenmechanik, Ruhr-Universität Bochum, Heft Nr. 32*, pp. 109–134.
- Wichtmann, T. (2005). Explicit accumulation model for non-cohesive soils under cyclic loading. Dissertation, Schriftenreihe des Institutes für Grundbau und Bodenmechanik der Ruhr-Universität Bochum, Heft 38.